AD-A039 846 NAVAL RESEARCH LAB WASHINGTON D C F/G 20/14
HIGH POWER MICROWAVES FROM A NON-ISOCHRONIC REFLECTING ELECTRON--ETC(U)
MAY 77 R A MAHAFFEY, P SPRANGLE, J GOLDEN

UNCLASSIFIED NRL-MR-3504 NL

| OF |
AD
A039846

END

DATE
FILMED
6-77

NRL Memorandum Report 3504

High Power Microwaves from a Non-Isochronic Reflecting Electron System (NIRES)

R. A. Mahaffey, P. Sprangle, J. Golden and C. A. Kapetanakos

Experimental Physics Branch
Plasma Physics Division

May 1977

NAVAL RESEARCH LABORATORY
Washington, D.C.

SECURITY CLASSIFICATION OF THIS PAGE *(When Data Entered)*

REPORT DOCUMENTATION PAGE

READ INSTRUCTIONS BEFORE COMPLETING FORM

1. REPORT NUMBER: NRL Memorandum Report 3504

2. GOVT ACCESSION NO.

3. RECIPIENT'S CATALOG NUMBER

4. TITLE *(and Subtitle)*: HIGH POWER MICROWAVES FROM A NON-ISOCHRONIC REFLECTING ELECTRON SYSTEM (NIRES)

5. TYPE OF REPORT & PERIOD COVERED: Interim report on a continuing NRL problem.

6. PERFORMING ORG. REPORT NUMBER

7. AUTHOR(s): R.A. Mahaffey*, P. Sprangle, J. Golden and C.A. Kapetanakos

8. CONTRACT OR GRANT NUMBER(s)

9. PERFORMING ORGANIZATION NAME AND ADDRESS
Naval Research Laboratory
Washington, D.C. 20375

10. PROGRAM ELEMENT, PROJECT, TASK AREA & WORK UNIT NUMBERS
NRL Problem H02-28A

11. CONTROLLING OFFICE NAME AND ADDRESS
Office of Naval Research
Arlington, Virginia 22217

12. REPORT DATE
May 1977

13. NUMBER OF PAGES
14

14. MONITORING AGENCY NAME & ADDRESS*(if different from Controlling Office)*

15. SECURITY CLASS. *(of this report)*
UNCLASSIFIED

15a. DECLASSIFICATION/DOWNGRADING SCHEDULE

16. DISTRIBUTION STATEMENT *(of this Report)*
Approved for public release; distribution unlimited.

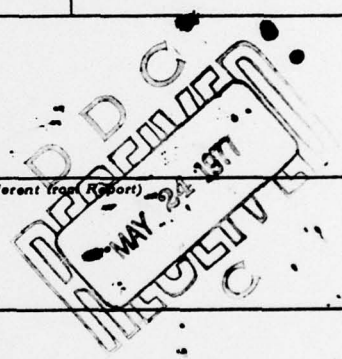

17. DISTRIBUTION STATEMENT *(of the abstract entered in Block 20, if different from Report)*

18. SUPPLEMENTARY NOTES
*NRC Research Associate at NRL.

19. KEY WORDS *(Continue on reverse side if necessary and identify by block number)*
High-power microwaves
Reflex triode
Non-isochronic electron systems

NRL-MR-3504

20. ABSTRACT *(Continue on reverse side if necessary and identify by block number)*
High-power microwave radiation of frequency 11 GHz and 36 HGz is observed when a 300 kV positive pulse is applied to an aluminized mylar anode of a reflex triode. The frequency of radiation varies as $f \sim V^{1/2}/d^n$, where V is the anode voltage, d the anode-cathode spacing and $0 < n < 1$. The basic features of the radiation are explained by a theoretical model based on the energy dependence of the electron oscillation frequency.

(square root of V)/(d to the n-th power)

DD FORM 1 JAN 73 1473 EDITION OF 1 NOV 65 IS OBSOLETE
S/N 0102-014-6601

SECURITY CLASSIFICATION OF THIS PAGE *(When Data Entered)*

251950

HIGH POWER MICROWAVES FROM A NON-ISOCHRONIC REFLECTING ELECTRON SYSTEM (NIRES)

Introduction

Reflecting electron systems in the form of a low inductance, coaxial reflex triode have been recently used successfully to produce MeV proton pulses[1] of peak current in excess of 200kA.

In this letter, we report results which demonstrate that, under suitable conditions, reflecting electron systems can also generate high power microwaves with or without an applied magnetic field (B_o). As will become apparent later on, reflecting electron systems have some distinct advantages over several of the previously reported devices that also use relativistic electron beams [2-8] for the generation of microwaves.

As shown in Fig. 1, in its simplest form, a reflecting electron system consists of a positively biased, semi-transparent anode and a grounded cathode[7]. Electrons emitted from the cathode are accelerated by the positive pulse that is applied to the anode, pass through it and form a virtual cathode. In general, the virtual cathode is formed at a distance from the anode that is different from the anode-cathode opening (d). As a result of the positive potential on the anode, the electrons do not leave the system but rather oscillate between the real and virtual cathodes.

The microwave emission is attributed to the phase bunching of the oscillating electrons inside the potential well of the system. This bunching is due to the energy (ε) dependence of the electron oscillation frequency ω_o. For the idealized parabolic potential well of Fig. 1b, ω_o is a function of ε only for relativistic electrons. In the presence of an oscillatory electric field $E = E_o \cos(\omega t)$ of frequency $\omega \gtrsim \omega_o$, a sample of initially uniformly distributed electrons will be

Note: Manuscript submitted April 22, 1977.

bunched as shown in Fig. 1c. The reason for this bunching is that $\partial\omega_o/\partial\varepsilon<0$ and thus those electrons located in the upper half plane at t=0 gain energy (ω_o decreases) and their phase slips behind the wave, while those at the lower half plane loose energy (ω_o increases) and their phase advances ahead of the wave. This non-isochronic mechanism is similar to that of the electron cyclotron maser[8,9].

The experimental set-up has been described previously in connection with the generation of intense, pulsed ion beams.[10,11] Briefly, the 50 nsec duration, 300-350 kV positive pulse from a 7-ohm generator is applied to the anode of a reflex triode. The anode is made either from 6 μm thick aluminized mylar or bare, parallel copper wires spaced 2 cm apart. It has been determined in previous experiments that with these sort of anodes the ion flux generated by the device is very small. Both the power and the frequency of the emitted microwaves appear to be sensitive to the shape of the cathode. The maximum power was obtained at $B_o = 0$ with a 8.4 cm OD solid cathode facing an aluminized mylar anode for d = 1.2 cm.

The emitted microwave radiation is monitored in both the X-band f =(8.2 - 12.4 GHz) and the Ka-band (f = 26.5 - 40 GHz). The horn-antennas are situated about 26 cm from the anode with their axis either parallel to the direction of the accelerating electric field (end-on) or with their axis perpendicular to it (side-on). A very small portion of the microwave signal taken from the output of a directional coupler which is located immediately after the horn is fed almost undispersed to an oscilloscope and is used as a time marker. The rest of the microwave signal is transmitted through a long (323 m in the X-band; 60 m in the Ka) dispersive line and is also fed to the same oscilloscope. The time

delay between the two signals gives information about the frequency spectrum of the radiation. Typical dispersed signals are shown in Fig. 2 together with the voltage pulse applied to the anode and the current flowing in the device. Since the power of the X-band radiation is about equal at the only two accessible positions of the system that are located about 90° apart, it is reasonable to assume that the emitted radiation is isotropic. Extrapolating the power measured at the horn under the above assumption the power emitted by the device at a single frequency over a 4π solid angle is between 90-100 MW, corresponding to an efficiency of about 1.5%.

A striking feature of the experimental results is the variation of the microwave frequency (f) with applied voltage (V) shown in Fig. 3. Clearly, the central frequency f_c of the spectrum varies as $f_c \sim \bar{V}^{\frac{1}{2}}$, where $\bar{V}$ is the time averaged anode potential. In addition, the results of Fig. 3 show that the frequency depends upon the shape of the cathode. It can be shown that the distance between the virtual cathode and anode decreases as the thickness of an annular cathode increases. Since the frequency of radiation $f \approx \ell \tau_t^{-1}$, where ℓ is an integer and τ_t is the transit time of a typical electron in the potential well, higher frequencies are expected with higher voltages and shorter openings between the real and virtual cathodes. As the anode is moved closer to the real cathode, the spacing between the anode and the virtual cathode is also reduced and thus higher frequencies are expected. This is shown in Fig. 4.

The voltage dependence of the microwave frequency can also explain the frequency spread of the signal shown in Fig. 2. For this particular

shot the voltage pulse drops by 150 kV during its duration, corresponding to a $\Delta V/V \simeq 0.4$ or to $(\Delta V/V)^{\frac{1}{2}} \simeq 0.2$, which is about equal to the observed $\Delta f/f$.

At $B_o = 0$, with an aluminized mylar anode located 1.2 cm away from a solid carbon cathode, the Ka-band power of the microwave radiation at the horn located about 26 cm from the anode with its axis parallel to the accelerating field is about 5 KW. This corresponds to a total power emitted over the 4π solid angle of more than 10 MW. Prior to detection, the signal is passed through a 60 m long dispersive line and the observed time delay of 230 nsec corresponds to a central frequency of 36.6 GHz.

A drastic reduction in the X-band microwave power is observed when the reflex triode is immersed in an external magnetic field. The emitted power shows a resonance-like behavior with the applied field. The power at the peak of the resonance is about two orders of magnitude lower than the corresponding power at $B_o = 0$. In addition, the frequency of the emitted radiation increases approximately linearly with the value of applied magnetic field.

To gain insight on the generation of the microwave radiation we have studied the dynamics of an ensemble of collisionless electrons that initially are distributed uniformly in phase inside an arbitrary potential well described by the electric field $E^{(o)}(z)$. It is assumed that at $t = t_o$ the system is perturbed by a small amplitude homogenous electric field $E^{(1)} = \hat{E} \exp(i\omega t)$. The equilibrium orbit of an electron ($E^{(1)} = 0$) is written in the form

$$z^{(o)}(t) = \sum_{\ell=-\infty}^{\infty} \hat{z}_\ell(\varepsilon) \exp\left\{ i\ell \left[\omega_o(\varepsilon) t + \varphi_o \right] \right\} ,$$

where $\hat{z}_\ell$ is the ℓth Fourier amplitude, ω_o is the fundamental oscillation frequency and φ_o is the initial phase of the particle. Note that ω_o and $\hat{z}_\ell$ are in general functions of the total equilibrium energy $\varepsilon = (\gamma^{(o)} - 1)m_o c^2 - |e|\phi^{(o)} = -\partial\phi^{(o)}/\partial z^{(o)}$. The change of the system's kinetic energy density due to $E^{(1)}$, averaged over φ_o for the $\ell=1$ mode is

$$\Delta W_{k.E} \equiv W_{k.E}(t) - W_{k.E}(t_o) = \frac{|e|2n_o\hat{E}^2\omega_o}{2(\Delta\omega_1)^2}\left[\omega_o\frac{\partial|\hat{z}_1|^2}{\partial\varepsilon}(1-\cos\Delta\omega_1\tau)\right.$$

$$\left. + |\hat{z}_1|^2\frac{\partial\omega_o}{\partial\varepsilon}\left\{(1+\frac{2\omega_o}{\Delta\omega_1})\{1-\cos\Delta\omega_1\tau) - \omega_o\tau\sin\Delta\omega_1\tau\right\}\right] , \qquad (1)$$

where n_o is the average electron density, $\Delta\omega_\ell = \omega - \ell\omega_o$, and $\tau = t - t_o$.

If $\Delta W_{k.E} > 0$ the perturbing wave is absorbed by the oscillating particles, while if $\Delta W_{k.E} < 0$ the particles lose kinetic energy to the wave resulting in wave growth. The term on the right hand side of Eq. (1) which contains the quantity $\partial|\hat{z}_1|^2/\partial\varepsilon$ is always positive and hence is a stabilizing term. The remaining term which is proportional to $\partial\omega_o/\partial\varepsilon$, however, can be negative depending on the sign of $\partial\omega_o/\partial\varepsilon$ and $\Delta\omega_1$. It is this term which gives rise to the growth of the wave. It can be shown from Eq. (1) that the condition for the initial growth of the wave is that

$$(\Delta\omega_1)^{-1}\partial\omega_o/\partial\varepsilon < 0, \qquad (2a)$$

together with

$$\frac{\partial|\hat{z}_1|^2}{\partial\varepsilon} < -\frac{|\hat{z}_1|^2}{\Delta\omega_1}\frac{\partial\omega_o}{\partial\varepsilon} . \qquad (2b)$$

The particle oscillations are non-isochronous, $\partial\omega_o/\partial\epsilon \neq 0$, if the potential well is non-parabolic and/or the particles are relativistic. In the present experiment both of these situations are satisfied. Using the wave equation for $E^{(1)}$ an approximate dispersion relation has been derived, which in the neighborhood of the unstable frequency takes the form

$$(\Delta\omega_1)^3 - \omega_b^2\omega_o m_o \frac{\partial}{\partial\epsilon}(\omega_o|\hat{z}_1|^2)\Delta\omega_1/2$$
$$= (\omega_b^2\omega_o^2 m_o |\hat{z}_1|^2/2)\,\partial\omega_o/\partial\epsilon\ , \qquad (3)$$

where $\omega_b^2 = 4\pi|e|^2 n_o/m_o$.

As an illustration we consider the simplified situation where the particles are mildly relativistic and the potential is parabolic given by $F^{(o)}(z^{(o)}) = \xi_o z^{(o)}$ where ξ_o is a constant. To lowest order in the small parameter $\epsilon/m_o c^2$ we find that

$$\omega_o = \alpha_o\left(1 - \frac{3}{8}\frac{\epsilon}{m_o c^2}\right),$$

and

$$|\hat{z}_1|^2 = \frac{c^2}{2\alpha_o^2}\,\frac{\epsilon}{m_o c^2}\ , \qquad (4)$$

where $\alpha_o = |e|\xi_o/m_o$ is the non-relativistic particle oscillation frequency in a parabolic potential. Using Eq. (4) in the expression for the dispersion relation we find that a threshold condition for instability exists and is

$$\epsilon/m_o c^2 > \frac{8}{9\sqrt{3}}\,\frac{\omega_b}{\alpha_o}\ . \qquad (5)$$

If the inequality in (5) is satisfied, Eq. (3) can be solved for the linear growth rate $\Gamma = -\mathrm{Im}(\Delta\omega_1)$ and frequency shift $\delta\omega = \mathrm{Re}(\Delta\omega_1)$, which are:

$$\Gamma = \frac{\sqrt{3}}{4}\left(\frac{3}{4}\right)^{1/3}(\omega_b^2\, a_o)^{1/3}\left(\frac{\varepsilon}{m_o c^2}\right)^{2/3} = \sqrt{3}\delta\omega \quad .$$

It is apparent from the previous discussion that NIRESes have four interesting features: (i) the emitted power is maximum when $B_o = 0$; (ii) compactness; (iii) tunability and (iv) monochromaticity. Thus, it is conceivable that they will lead to the development of practical, high frequency microwave sources in the future.

It is very likely the mechanism responsible for the generation of microwave radiation in our system is also responsible for the high power (more than 1 GWatt) X-band radiation observed by Doucet and Buzzi[12], when a 400 kV, 200 kA relativistic electron beam is injected into a vacuum through a foil anode.

References

*NRC Research Associate at NRL.

1. J. Golden, C.A. Kapetanakos, S.J. Marsh and S.J. Stephanakis, Phys. Rev. Lett., 38, 130 (1977).
2. J.A. Nation, Appl. Phys. Lett. 17, 491 (1970).
3. M. Friedman and M. Herndon, Phys. Rev. Lett. 28, 210 (1972).
4. M. Friedman, D.A. Hammer, W.M. Manheimer and P. Sprangle, Phys. Rev. Lett. 31, 752 (1973).
5. N. I. Zaytsev et al. Radiotekhmika i Electronica, 19, 1056 (1974).
6. V.L. Granatstein, P. Sprangle, R.K. Parker and M. Herndon, J. Appl. Phys. 46, 2021 (1975).
7. S. Humphries, T.J. Lee and R.N. Sudan, Appl. Phys. Lett. 25, 20 (1974).
8. A.V. Gapanov, M.I. Petelin and V.K. Yulpatov, Izv. VVZ. Radiofizika 10, 1414 (1967).
9. P. Sprangle and A.T. Drobot, IEEE Special issue on sub-milimeter rad. p. 65, June, 1977 (and references therein).
10. C.A. Kapetanakos, J. Golden and F.C. Young, Nuclear Fusion 16, 151 (1976).
11. J. Golden and C.A. Kapetanakos, Appl. Phys. Lett. 28, 3 (1976).
12. H.J. Doucet and J. Buzzi, Private communication.

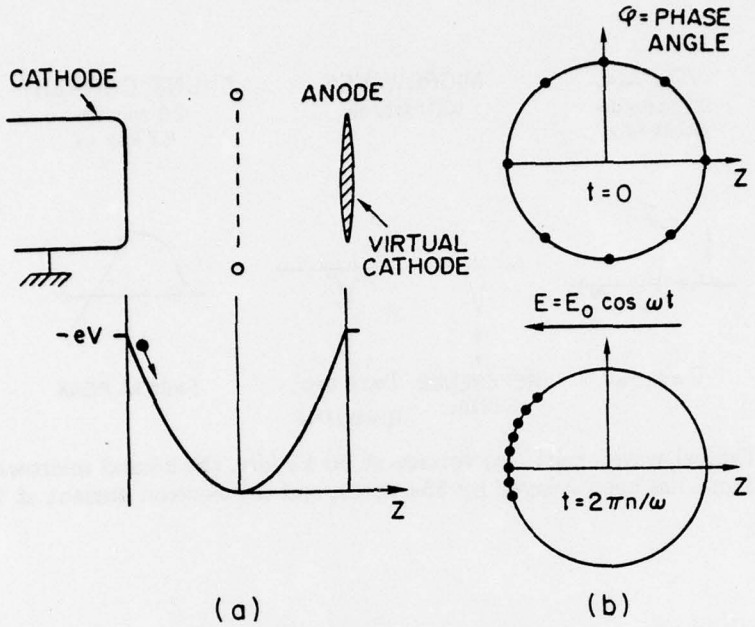

Fig. 1 — (a) Reflex triode and idealized potential well, and (b) phase bunching of electrons after several periods when $\omega \gtrsim \omega_o$

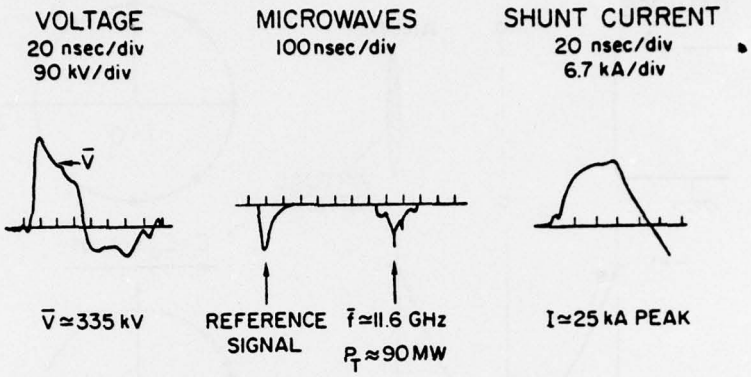

Fig. 2 — Typical waveforms: (a) voltage at 90 kV/div, (b) x-band microwaves, (the reference signal has been delayed by 554 nsec), and (c) electron current at 7 kA/div.

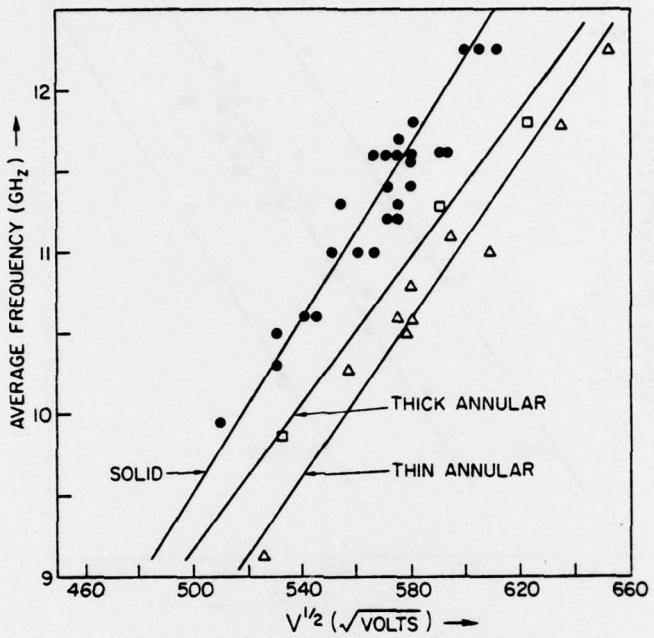

Fig. 3 — Average frequency vs. the square root of the averaged applied voltage for three different cathodes of area: 55 cm^2 (solid); 89 cm^2 (thick annular); and 51 cm^2 (thin annular).

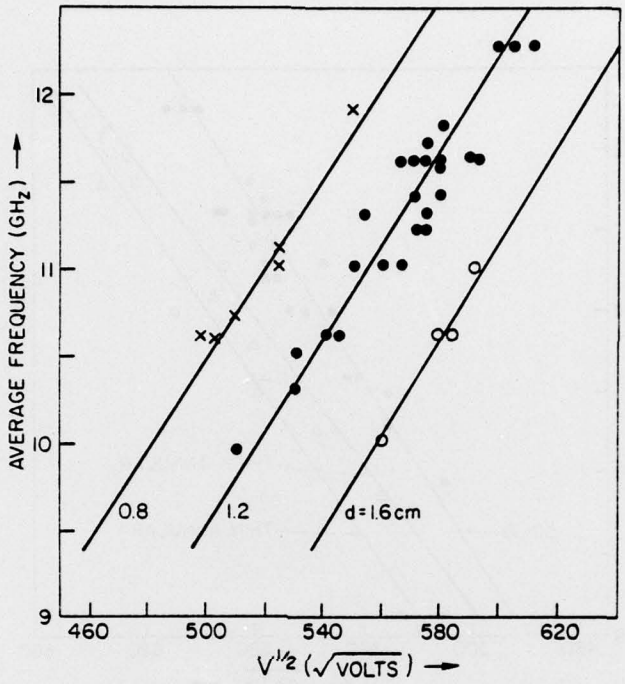

Fig. 4 — Average frequency vs. the square root of the averaged applied voltage for three anode-cathode spacings